Sensors and Materials, Vol. 34, No. 6 (2022) 2403–2425
MYU Tokyo

S & M 2980

Sarcopenia Recognition System Combined with Electromyography and Gait Obtained by the Multiple Sensor Module and Deep Learning Algorithm

I-Miao Chen, Pin-Yu Yeh, Ting-Chi Chang, Ya-Chu Hsieh, and Chiun-Li Chin*

Department of Medical Informatics, Chung Shan Medical University,
No. 110, Sec. 1, Jianguo N. Rd., Taichung City 40201, Taiwan

(Received December 27, 2021; accepted May 31, 2022)

Keywords: wearable sensors, MSM, EAG, Bodi algorithm, gait indicators, LCNet

At present, many diseases can be predicted through data obtained by wearable sensors. The majority of these proposed wearable devices only use inertial sensors to obtain the walking motion signals of a subject. However, since the symptoms of sarcopenia are reflected in the changes in human muscles, we propose a sarcopenia recognition system, which consists of hardware and software. The hardware is composed of multiple sensor module (MSM), which is a wearable device used to collect the signals of electromyography and gait (EAG). The software is composed of biomedical and inertial sensors algorithm (Bodi algorithm) and leg health classification net (LCNet). The Bodi algorithm is used to calculate various gait indicators after predicting the risk of sarcopenia obtained by LCNet. The accuracy of LCNet is 94.41%, its precision is 91.58%, its specificity is 95.81%, and its sensitivity is 91.58%. In the future, we expect to use the proposed MSM to collect additional subjects' gait data and apply it to other disease predictions to assist physicians in disease diagnosis.

1. Introduction

In the field of clinical diagnosis, the use of low-cost, portable, and wearable sensors for human activity measurement has become a very common detection method. Among wearable sensors, frequently used devices include inertial sensors such as accelerometers or gyroscopes, electromyogram (EMG) sensors such as biomedical signal sensors, ground reaction force (GRF) sensors, and others. The current research is generally limited by the sensors' energy consumption; thus, few sensors are generally used for human activity and gait measurement.(1) As a result, the gait data collected by the sensors can only be used to determine some gait parameters. For example, inertial sensors can only be used for collecting the human body's movement direction but cannot be used to interpret the electromyographic signals generated by human muscle activity; therefore, we can only calculate gait parameters using sensor values such as step length, stride length, and walking speed, but the changes in muscle strength cannot be calculated using gait data.

*Corresponding author: e-mail: ernestli@csmu.edu.tw
https://doi.org/10.18494/SAM3787

ISSN 0914-4935

Furthermore, wearable sensors are currently used in many studies to collect human gait data, and they have been widely used in the fields of gait analysis, disease prediction, health re-evaluation, and medical care.[2,3] In the wearable sensor application range, gait parameters are generally calculated using gait data and are used to assess whether the subject exerts uneven forces on the left and right feet or the asymmetry of the left and right feet; additionally, the step parameters can predict the probability of suffering from scoliosis, sarcopenia, Parkinson's disease,[4] and multiple sclerosis.[5] Among them, sarcopenia is a disease that has attracted considerable attention in recent years. It is evidenced by decreased muscle quantity and muscle function decline. However, malnutrition, insufficient physical activity, and chronic diseases can also lead to the occurrence of sarcopenia. Moreover, in the current preliminary assessment of sarcopenia, doctors often use three factors, namely, human muscle strength, muscle quantity, and physical performance, to determine whether there is a risk of sarcopenia.[6–7] However, professional instruments are not used to calculate these indicators when implementing testing, and most diagnoses are based on the doctor's experience. In addition, there are many test items, and the patient must repeat similar tests many times before the physician can determine whether the patient has sarcopenia and its severity.

Given the above problems, we developed a multiple sensor module (MSM) that has a low power consumption and uses a small Arduino Nano 33 BLE Sense as the micro-control processing core, combined with a built-in accelerometer, an EMG sensor, lithium batteries, and lithium battery charging boards. These components are used to collect electromyography and gait (EAG) signals, which consist of three-axis acceleration and myoelectric signals during walking to analyze a person's health status.[8–10] Then, we calculate gait indicators such as step length, stride length, walking speed, and muscle strength using the Bodi algorithm proposed in our study. The Bodi algorithm can be used to discover a subject's problems when walking, such as whether the subject distributes weight to one side of the body, and it also provides gait indicators that assist the physician in assessing the subject's health. In addition, we also input the calculated gait indicators into a deep learning model for training so that it can learn to recognize and predict the risk of sarcopenia. Therefore, people may pay more attention to skeletal muscle mass loss and go to the hospital for further examination before symptoms become severe.

This study is divided into four sections. In Sect. 2, we discuss the related literature. In Sect. 3, we introduce this study's research methods, including the system process, software, developed hardware devices, self-collected gait dataset, model, and algorithm used in this study. Sect. 4 consists of the experimental results and provides a discussion regarding the different variables. In the final section, we present the conclusion and future research directions.

2. Related Works

2.1 Application fields of wearable devices and importance of gait parameters for health prediction

Many studies have collected human activity signals using small and portable wearable sensors. In 2012, Tao *et al.* mentioned that the gait analysis methods based on wearable sensors

can be divided into three categories, namely, gait kinematics, gait kinetics, and electromyography.(2) In gait kinematics, inertial sensors such as accelerometers and gyroscopes are often used to collect dynamic gait data and are installed on the waist, thighs, or calves of the human body to measure acceleration or angular displacement while walking. In electromyography, EMG sensors are primarily placed on the skin's surface to measure the human body's EMG signals when walking, such as the muscle change between steps, which can also be used to calculate muscle strength. However, EMG sensors must be placed in a specific position on the muscle before they can be used as a gait analysis tool for clinical treatment when assessing the recovery degree of patients with neurological diseases such as Parkinson's disease and stroke.(2)

Additionally, in 2020, Díaz *et al.*(1) mentioned sensors in wearable sensor systems, such as an inertial measurement unit (IMU) and electromyography (EMG) sensors, which are commonly placed on the breastbone, waist, or upper and lower limbs to assess balance disorders and measure gait parameters. The wearable sensors play an important role in rehabilitation research and have the advantage of realizing gait characterization and the objective evaluation of balance function performance. However, the sensors' power consumption is currently a major problem in this field. The more sensors are used, the more power the system consumes, which may cause the system to fail to achieve the expected performance. Therefore, this problem is also a focus of future research.

In 2019, Gujarathi and Bhole(11) placed two inertial MPU6050 sensors, which include a three-axis accelerometer and a gyroscope, on the lower leg to assess and monitor the rehabilitation degree of orthopedic patients; they also used the sensors to collect the subjects' gait signals during a 40 m walk. Then, they used the gait analysis algorithm to calculate gait parameters such as the stride length, step length, and standing time, among others. In this study, we found that acceleration and gyroscope signals can be used to evaluate the degree of rehabilitation. However, the sensor must be equipped with an Arduino Uno micro-control board to collect gait signals. Therefore, when the user wears this device while walking, the walking state may be affected by the collection device's large size, resulting in unobjective data.

In 2010, to explore the relationship between age and lower extremity muscle EMG signals and electromyography, Tian *et al.*(12) placed EMG and mechanomyography (MMG) sensors on the subjects' quadriceps femoris muscles to collect the signals. The experimental results prove that results from the elderly are not as good as those from the young in terms of EMG or MMG signals. This result means that muscle strength decreases with increasing age and is related to muscle quantity. Then, in 2011, Kashiwagi *et al.*(13) placed surface electromyography (SEMG) sensors on the subjects' left and right erector spinae to collect the four waist movements of the human body, namely, forward, backward, left, and right, and to detect the potential changes of the erector spinae EMG signals to help nursing staff understand the patients' condition and complete nursing tasks quickly. The above study demonstrates that the EMG sensor is placed on the skin surface at a specific muscle position, and then the surface EMG signal is measured by the EMG sensor. The results not only help researchers and medical professionals understand human muscle contractions and movement, but can also be used to understand human health.

2.2 Gait data processing and indicator calculation and application

The world has gradually entered an aging society, and as a result, the problem of human aging has attracted increasing attention. In 2019, Bonetto and Bonewald[14] mentioned that if accompanied by age-related bone loss, decreased muscle quantity and symptoms related to loss of function can be called sarcopenia, which generally becomes prevalent once patients surpass the age of 30, and after they surpass 60 years of age, the muscle quantity will decrease rapidly. Additionally, they mentioned that 20% of the global population over 60 years old will suffer from sarcopenia in 2050, which demonstrates its importance. In the same year, Cruz-Jentoft *et al.*[6] elaborated on the EU sarcopenia working group to update the definition and diagnostic criteria of sarcopenia and mentioned that, in addition to aging, sarcopenia can also be caused by decreased mobility, such as that which occurs during long-term bed rest. Both young and old patients have a chance of suffering from sarcopenia. In clinical diagnostic criteria, it is also mentioned that the human body's muscle strength, muscle mass, and physical performance can be used to diagnose the presence of sarcopenia as well as its severity. In 2020, Chen *et al.*[7] explained in detail the diagnostic criteria for sarcopenia revised by the Asian Working Group for Sarcopenia (AWGS). They also noted the hereditary difference between Asians and Europeans in terms of body shape and lifestyle, which causes a problem because the judgment standard established by the European Working Group on Sarcopenia in Older People 2 (EWSGOP2) does not apply to Asians. However, in the current sarcopenia diagnostic process, professional medical equipment that can provide measured values for physician reference is only available for muscle quantity. There is no easy-to-operate measurement tool with a consistent judgment standard for measuring muscle strength and physical function when diagnosing sarcopenia.

Gait analysis is one of the methods used to evaluate patient behavior and motor function in clinical medicine. To help medical staff quantify patients' physical activity, many studies have used wearable devices to collect human activity signals and have proposed methods to quantify gait data. In 2006, Alvarez *et al.*[15] compared five mathematical estimation models for calculating the step length and converted the gait data collected by the accelerometer to provide a more accurate step length evaluation model. Then, in 2011, Jin *et al.*[16] proposed a relative threshold detection method to find the peak and valley values in the acceleration data to infer the location of pedestrians using low-cost sensors built into smartphones, such as accelerometers or digital compasses. However, in this study, we demonstrate that accelerometers are susceptible to noise from irregular activities by the human body. In 2015, Lan *et al.*[17] proposed a Pedestrian Dead Reckoning (PDR) attitude estimation method based on inertial sensors and satellite navigation systems to track pedestrian positions, and the peak and valley values from the acceleration data were also used to infer the pedestrians' number of steps and step length. The results prove that this calculation method can effectively ascertain pedestrians' walking direction and distance.

In 2012, Kuriki *et al.*[18] placed electrodes on the surface of the skin to detect EMG signals to infer muscle strength, but by only collecting EMG signals, muscle strength cannot be evaluated. Therefore, they combined this strategy with signal correction methods or standardized instruments and methods, such as root mean square (RMS) and principal component analysis

(PCA), among others. To explore the correlation between EMG and muscle strength, we use the RMS method to quantify the EMG signal. The results show that the EMG signal increases with muscle contractility and that the amplitude of the EMG signal related to isometric or isotonic contraction increases with the square root of the signal. In the study discussed above, Díaz *et al.*[1] mentioned not only the types and application fields of common wearable sensors but also the evaluation indicators and algorithms of gait parameters, such as the calculation formulas of step length, stride length, and walking speed.

PDR uses the kinematic characteristics of pedestrian gait, travel distance, and walking direction data. It is primarily composed of three important components, namely, step length detection, stride length estimation, and walking direction estimation, and it uses an accelerometer to detect a pedestrian's step length to provide accurate and continuous navigation results for pedestrian navigation.

2.3 Application of machine learning and deep learning to human activity classification and prediction

In recent years, the application of machine learning and deep learning in medical treatment has increasingly matured, and better disease prediction and analysis will be realized by combining human activity data and machine learning or deep learning methods. In 2018, Zebin *et al.*[19] used the LSTM architecture to classify the data collected by an accelerometer and a gyroscope into six daily activities, and the accuracy is 92%. It can be seen that LSTM can achieve a good classification effect for a continuous-time signal. However, the classification effect of the discontinuous-time signal was not mentioned. In 2019, Alharthi *et al.*[3] integrated the methods of gait monitoring, gait feature extraction, and analysis, but most of the studies rely on manual gait feature extraction, which is prone to errors. It has been found that using deep learning to automatically extract gait features can eliminate dependence on handcrafting; it can also build a fall or disease prediction system. In the same year, Côté-Allard *et al.*[20] used the concept of transfer learning to train the ConvNet deep learning model to classify the one-dimensional data in the Myo Armband and NinaPro datasets, such as the original EMG signal, the spectrogram of the EMG signal, and the continuous wavelet transform (CWT) EMG signal data. These data can also be used to identify the gesture of the subjects. In addition, the classification accuracy of the ConvNet model can reach 98.31%, which means that it can classify different gestures accurately from the electromyogram.

According to multiple studies, wearable devices are often used to collect human activity signals and predict diseases, and as a human health assessment tool. However, most of the studies only use a single sensor to collect the subjects' human activity signals, and they rarely combined the inertial and EMG sensors to collect the subjects' acceleration and EMG signals for analysis. It is easy to neglect the importance of acceleration or EMG signals for gait and health prediction. In addition, there are still a few studies that use deep learning models for disease risk assessment and the prediction of calculated gait indicators. Therefore, we use the small and low-cost Arduino Nano 33 BLE Sense with low power consumption and inertial sensors as the primary control core for the "wearable detection box", which can improve the energy

consumption of the hardware as well as widen the range of the Bluetooth connection. Then, we refer to the installation position of the wearable sensor mentioned in the above study and install the SEMG sensor in MMG on the left and right erector spinae muscles of the human body and place the accelerometer on the quadriceps of both feet to facilitate the collection of gait signals during the test project. Next, we refer to the gait index calculation method mentioned above to analyze and process human activity and gait signals collected by accelerometers and EMG sensors. Finally, according to the above literature, although the recurrent neural network (RNN) performs well in classifying continuous-time data, the data pre-analyzed in this study are an indicator of discontinuous time. Therefore, we proposed a leg health classification net (LCNet) and input the gait indicators into the LCNet deep learning model for training. Not only can it be used in the early prediction of diseases, but it can also be used as a diagnostic reference for physicians. The contribution of this study lies in the following.

(1) The MSM proposed in our study combines an accelerometer and EMG sensors, so the collected gait data provide more diverse gait indicators as a basis for assessing health status.
(2) We install MSM at specific locations on the human body, such as the waist, thighs, and calves, which means that we can collect more meaningful human activity signals.
(3) We input the calculated gait indicators into the deep learning model for training to achieve sarcopenia risk predictions.

3. Materials and Methods

In this study, we use MSM to collect the subjects' EAG signals, which consists of three-axis acceleration and myoelectric signals during the test. Next, we use the Bodi algorithm proposed in this study to calculate gait indicators such as the step length, number of steps, and pace. Finally, we input the gait indicators calculated using the Bodi algorithm into LCNet to classify the risk of suffering from sarcopenia. Figure 1 shows this study's flowchart, which is primarily divided into two parts, namely, the testbed system and the proposed analysis method. We have built a testbed system that uses the interface for connecting multiple sensor modules (ICMSM) to connect to the MSM installed on the subject via BLE to collect data. In the testbed system, we also introduce MSM, ICMSM, and participation and experiment protocols. Next, in the description of the proposed method, we introduce the Dataset, Data Augmentation, Data Normalization, the Bodi algorithm proposed in this study, and LCNet.

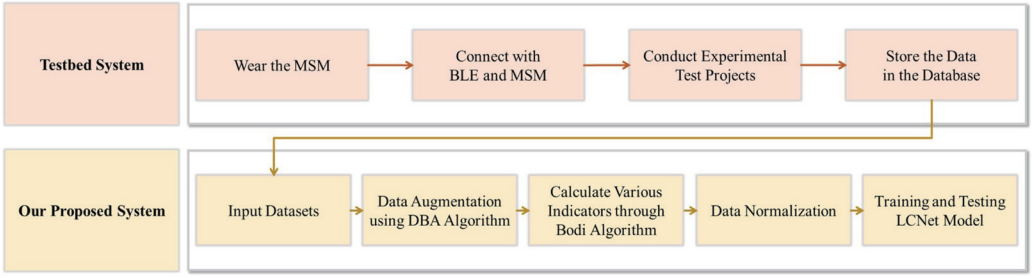

Fig. 1. (Color online) Flowchart of our proposed system.

3.1 MSM

To collect human gait performance data, we have built a testbed system that can obtain the EAG signals of humans from wearable devices. Each MSM includes a sensing module, a communication module, a microcontroller module, and a power module. The MSM circuit and architecture diagrams are shown in Figs. 2(a) and 2(b).

In the sensing module, we use an inertial sensor and a biomedical signal sensor. We adopt the LSM9DS1 chip in Arduino Nano 33 BLE Sense as an inertial measurement unit (IMU) to obtain the subject's three-axis accelerations while walking, sitting, and getting up, which are the *X*-axis, *Y*-axis, and *Z*-axis accelerations, respectively. Then, we adopt the EMG Detector as a biomedical signal sensor to collect the electrical signals from muscle contraction during walking, sitting, and getting up. This device processes the received signal four times, which includes two amplifications and two filterings.

To reduce the load of the power module in the wearable device, we use the Bluetooth Low-Energy Module for data transmission, as well as the Bluetooth Low-Energy Chip, which is embedded in the Arduino Nano 33 BLE Sense. We use Bluetooth to transfer the data received by the sensor module to the connected mobile device and to store the data in the server.

To reduce the size of the wearable device, we adopt Arduino Nano 33 BLE Sense as the microcontroller module, which has an embedded communication module and an inertial sensor. The microcontroller module is connected to the sensing module, which defines the period over which the sensing module receives data and transmits it to the mobile device.

To power the entire circuit, we use a 3.7 V lithium polymer battery to supply power and we also add a lithium battery charging protection board. The battery is connected in parallel to the Arduino Nano 33 BLE Sense and EMG Detector. The operating voltages of the Arduino Nano 33 BLE Sense and EMG Detector are both 3.3 V, so this power module can effectively supply the entire circuit's power demand.

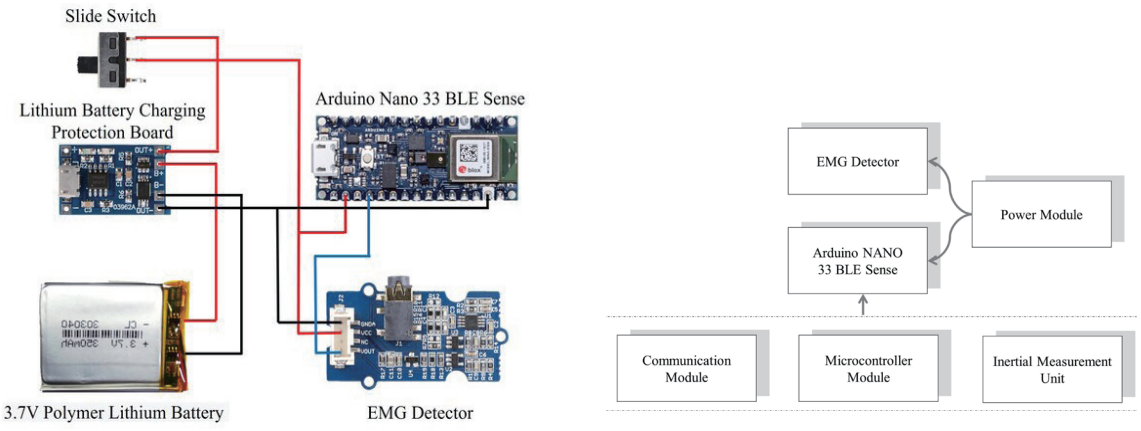

(a) (b)

Fig. 2. (Color online) (a) MSM circuit diagram. (b) MSM architecture diagram.

3.2 ICMSM

To collect the gait data detected by MSM, we have built a testbed system. On the front end, we used HTML5, which is low-cost and cross-platform combined with JavaScript, which is highly interactive to complete the Web App interface. The testbed system interface and architecture is shown in Fig. 3. This configuration means that regardless of the operating system, such as iOS or Android, all users can access the Web App through a browser. To complete the communication between software and hardware, we use the Web Bluetooth API to enable the browser to obtain the data transmitted by the Bluetooth Low-Energy Device. At the same time, we present the data in the experimental interface. Next, we use the Web Storage API to temporarily store the data in the browser, encapsulate it once 50 data points have been collected, and then use Ajax technology with the PHP back-end programming language to transfer the data to the MySQL database. This strategy avoids losing data due to sending too much data at the same time.

3.3 Participation

We collected activity data from 19 researchers working in a research institute and their families. There were 55 subjects in total. All subjects consented to participate. The subjects consisted of 21 men and 34 women, aged between 20 and 81, weighing between 38 and 112 kg, and having a skeletal muscle mass between 12 and 29 kg. Patients with severe leg or spine injuries were excluded. Among the effective subjects, we defined 19 subjects as being at high risk of sarcopenia according to the diagnostic method proposed in a previous study,[6] which is based on the subjects' calf circumference and skeletal muscle mass. The remaining 36 subjects were defined as the low-risk group. Table 1 shows the descriptive statistics.

3.4 Experimental protocols

To understand the subjects' physical performance, we use the sarcopenia diagnostic criteria proposed by the European Working Group on Sarcopenia[6] and asked each subject to take the

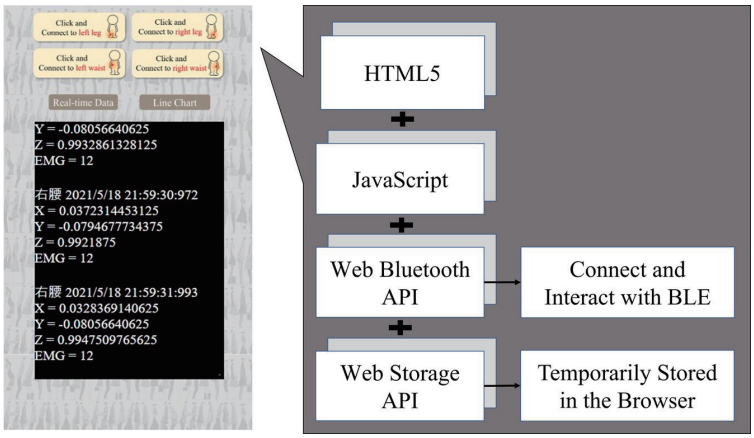

Fig. 3. (Color online) Testbed system interface and architecture.

Table 1
Descriptive statistics.

	Mean	Min	Max	Range
Age	33.88	19.00	81.00	62.00
Weight	62.33	38.00	112.00	74.00
Skeletal muscle	18.83	12.50	28.99	16.48

Four-meter Usual Walking Speed Test and the Time-up and Go Test six times. In most human gait kinematics measurements, the accelerometers are worn on the thighs and calves[2] to collect gait data during the test, and the accelerometer placed on the waist can obtain data about the gait cycle. Therefore, we will place the MSM at the back of the left and right legs and at the back of the subject's waist. To obtain the subject's muscle activity while walking, we attach the electrode patches of the EMG Detector to the left and right erector spinae muscles.[13] To obtain data about waist movement during walking and the changes in thigh muscle contraction during walking, sitting, and getting up, we attach the electrode patches to the quadriceps femoris muscles of the left and right thighs. The positions at which the MSM is worn are shown in Fig. 4, and the directions of the *X*-axis, *Y*-axis, and *Z*-axis of each MSM are uniform. Each subject was asked to walk normally during the test, with no requirement to walk fast or slow. At the same time, the entire test process is monitored by researchers, and the walking time is calculated.

3.4.1 Four-meter Usual Walking Speed Test

Since the Four-meter Usual Walking Speed Test is considered to most resemble daily walking, it is one of the important tests used to evaluate walking speed in the related literature.[6] In this test, the subject starts with a standing posture and then walks straight for four meters at a normal walking speed. The schematic diagram of this test is shown in Fig. 5.

3.4.2 Time-up and Go Test

The Time-up and Go Test is a test that can measure the soundness of the functions required for human movement in all aspects.[6,7] During the test, the subject needs to start at a sitting state, then gets up and walks three meters. Next, the subject turns 180 degrees, walks back to the starting point, and sits down. Since the test consists of getting up from a chair and turning around, the test is also regarded as a measure of muscle function. A schematic diagram of the Time-up and Go Test is shown in Fig. 6.

3.5 Dataset

In this study, we collected various data about the subjects' walking during the two tests using inertial sensors and biomedical signals, including their *X*-axis, *Y*-axis, *Z*-axis accelerations, and EMG. There are a total of 55 subjects in the test, and each test collects six valid data. To ensure the validity of the received data and to avoid losing data during exchange and transmission due to environmental interference, the data sampling rate used was 6 Hz. Finally, a total of 660 valid

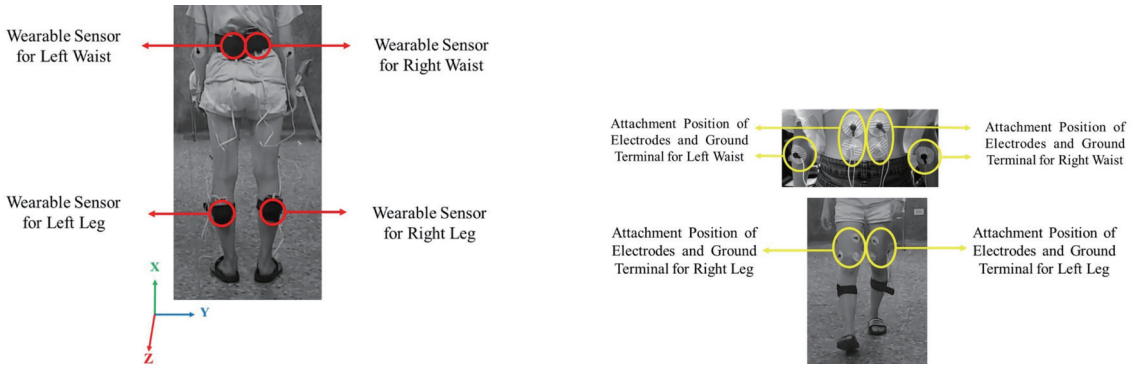

(a) (b)

Fig. 4. (Color online) (a) Positions at which MSM is worn on the body. (b) Positions where electrodes and ground terminal are attached.

Fig. 5. (Color online) Schematic diagram of Four-meter Usual Walking Speed Test.

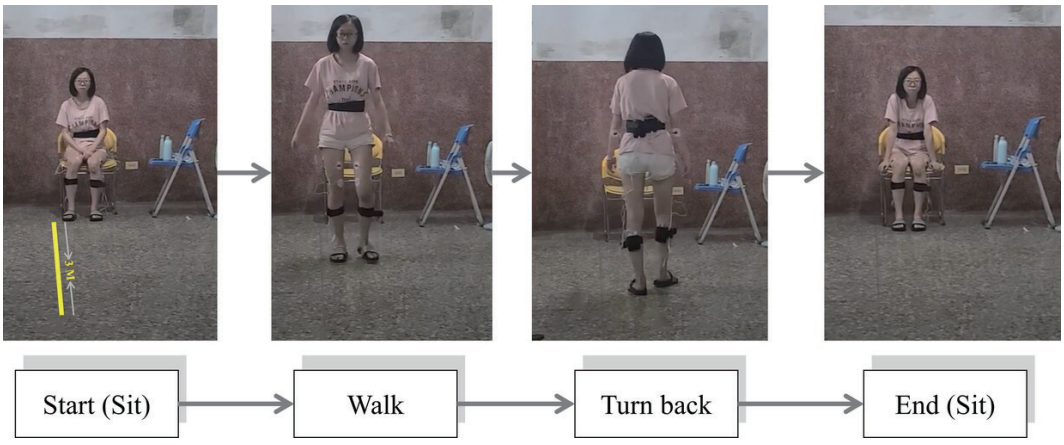

Fig. 6. (Color online) Schematic diagram of Time-up and Go Test.

data points were obtained in the two tests. In the denoising part, we used the median filter to filter noise in the raw data.

3.6 Data augmentation

As a small number of data cause the model to overfit, data augmentation allows the model to learn more about the characteristics of data invariance. Therefore, we adopt the DTW

Barycenter Average (DBA) algorithm, which was developed specifically for time series,[21–23] to improve the model's generalization ability. Finally, the amplified dataset has a total of 2860 data points. In this study, 90% of the time-series data in this dataset is used as the training dataset, and 10% is used as the test dataset.

3.7 Bodi algorithm

To assist rehabilitation physicians in clinical diagnosis and disease analysis, we calculate the indicators from the data obtained by the MSM. Among the indicators used in this study, seven indicators are calculated on the basis of three-axis acceleration signals collected by the inertial sensor: step length, stride, the number of steps, step speed, average acceleration, acceleration RMS, and symmetry. The other two indicators are calculated on the basis of the data from the biomedical signal sensor, which includes the average EMG and EMG RMS.

3.7.1 Indicators calculated on the basis of three-axis acceleration signals

Step length represents the distance between the feet when both feet are on the ground. When the step length is large, the leg has to expend more power to step, which expresses the strength of the leg muscles.[1,15–17] To calculate the step length, we first obtain the acceleration in the forward direction. In this study, the subject's forward direction is the *Z*-axis of the inertial sensor. Then, we find the maximum and minimum values of the *Z*-axis acceleration. The step length is defined as

$$Step = (Z_{max} - Z_{min})^{1/4}. \tag{1}$$

Z_{max} and Z_{min} represent the maximum and minimum values of the *Z*-axis acceleration, respectively.

Stride is defined as the distance between the two right heels, that is, the sum of the lengths of the left and right feet. It is mainly affected by the muscles' horizontal and vertical forces, which means that insufficient muscle strength or the wrong direction of the force will affect the stride size. The stride equation is

$$Stride = Step_{left} + Step_{right}. \tag{2}$$

$Step_{left}$ and $Step_{right}$ represent the step lengths of the left and right feet, respectively.

After knowing the step length and stride, we can calculate the number of steps, which is closely related to the step size.[24] However, the step size is closely related to the muscle strength; that is, the smaller the number of steps, the larger the step length and the greater the effort required to walk and stride. Therefore, it can be used to express the leg muscle strength. The number of steps is defined as

$$Num = |\, Distance / (Stride / 2) \,|, \tag{3}$$

where *Distance* is the testing distance.

Gait speed, also called walking speed, is the distance walked in a given period. Walking speed represents the overall walking performance, that is, it can be used to measure the ability, reliability, and sensitivity of assessing and monitoring overall health. The gait speed equation is

$$Speed = \left[Num / \left(Time / 60 \right) \right] \times Stride \times 0.5. \tag{4}$$

Num and *Time* represent the total number of steps and the total time taken during the test, respectively.

In addition to the indicators related to pace, we also calculated the indicators related to directionality. The subject may move in different directions during the test, the acceleration value in a single direction cannot stably reflect the subject's gait performance, and the axis perpendicular to the ground has a higher value than the other two axes.[25] To avoid arbitrary movement by a subject as well as the effect of a single axis on other axes, we perform the following processing on the three-axis acceleration:

$$TA = \left(Acc_x{}^2 + Acc_y{}^2 + Acc_z{}^2 \right)^{0.5}, \tag{5}$$

where Acc_x, Acc_y, and Acc_z represent the accelerations of the *X*-, *Y*-, and *Z*-axes, respectively.

The human waist is very close to the human body's center of mass when standing: thus, the acceleration signals collected at that position can effectively capture changes in a subject's gait. In addition, there is a nonlinear relationship between RMS and walking speed;[26] thus, the RMS acceleration is calculated as

$$RMS_{Acc} = (\frac{1}{n}\sum_{j=1}^{n} Acc_j{}^2)^{0.5} \times Speed^{-2}, \tag{6}$$

$$TRMS_{Acc} = RMS_{Acc\_x} + RMS_{Acc\_y} + RMS_{Acc\_z}, \tag{7}$$

where *n* is the number of data collected, *Acc* is the acceleration of the *X*-, *Y*-, or *Z*-axes, and *TRMS* is the *RMS* of the total acceleration.

Finally, to assess whether the subject is coordinated on the left and right sides during human activity and to observe whether there is unilateral damage to the leg,[27] we calculate the symmetry of the gait parameter. In this study, we utilize the average acceleration as a parameter to evaluate symmetry. When $S = 0$, the left and right sides are completely symmetrical. When *S* is larger, the left and right sides are more asymmetrical. The symmetry evaluation equation is

$$S = \frac{\left| A_L - A_R \right|}{0.5 \times \left(A_L + A_R \right)}, \tag{8}$$

where A_L is the average acceleration of the left waist or left foot, and A_R is the average acceleration of the right waist or right foot.

3.7.2 Indicators calculated on the basis of EMG signals

EMG is a muscle activity sensing technology that detects the transmission of human nerve signals and changes in muscle contraction. However, EMG signals are susceptible to noise interference. Therefore, the signal processing or calculation of related indicators is required to easily observe muscle activity.[28] Therefore, we calculated the average EMG for the subject's four body parts in one test. The calculation formula is

$$EMG_{avg} = \frac{1}{n}\sum_{j=1}^{n} EMG_j, \tag{9}$$

where n is the number of EMG_s and EMG_j is the value of EMG.

EMG RMS represents the amplitude of the EMG signal, and the EMG signal amplitude increases with the muscle contractility. Additionally, the EMG signal amplitude of isometric or isotonic contraction is expected to increase with the square root of the signal. This relationship can be used to evaluate the force exerted by the muscle strength. The calculation equation for EMG *RMS* is

$$RMS_{EMG} = \left[\left(\sum_{i=1}^{n} x_i^{\,2}\right) \times n^{-1}\right]^{0.5}, \; i = 1,2,3,\ldots,n, \tag{10}$$

where n is the number of data collected and x is the EMG value.

3.8 Data normalization

Since the unit of each indicator is different, the value range between the indicators may be very large. Therefore, we normalize each indicator separately to narrow the range gap so that the model will not be affected by the value range of the indicator during model training. The gap is unbalanced and affected. We use Eq. (11) to normalize the indicator:

$$X_{normalize} = \frac{X_i - \overline{X}}{\sigma_x}, \tag{11}$$

where X_i is the value of each indicator, $\overline{X}$ is the average of all the indicator values, and σ_x is the standard deviation of all the indicator values.

3.9 LCNet

LCNet is a deep learning model used to classify one-dimensional signals, which can be well applied to the analysis of time series data collected by sensors, including inertial and biomedical signal sensors.[29,30] Figure 7 shows the LCNet architecture. The LCNet proposed in this paper is used to classify the risk of sarcopenia. There are two categories, namely, a low risk of sarcopenia and a high risk of sarcopenia. This model is primarily composed of a convolutional layer and two fully connected layers. Then, we input the gait parameter calculated using the Bodi algorithm into the convolutional layer. The kernel size is 1 × 3. To improve the model training speed and the model's ability to deal with nonlinear problems, we use ReLU as the activation function. Finally, the fully connected layer outputs the classification result. In this study, we use SGD as the optimizer for model training, and the model's classification result is better when the learning rate is 10^{-4}, the batch size is 30, and the network is trained for 3500 epochs.

4. Experimental Results

In this study, we use a computer with 32 GB of RAM, an i7-9750H CPU, and an NVIDIA GTX 1060Ti GPU to train the LCNet model, which was developed by the Keras framework.

4.1. Model performance analysis

To evaluate the classification ability of the LCNet model, we adopt the confusion matrix to evaluate the model's classification; that is, the confusion matrix clearly shows the correct and incorrect classifications for each type of sample. A confusion matrix is primarily composed of 4 elements, namely, True Positive (TP), True Negative (TN), False Negative (FN), and False Positive (FP). TP means that the actual value and the model's classification results both indicate a high risk of developing sarcopenia. TN indicates that the actual value and the model's classification results both indicate a low risk of developing sarcopenia. FN refers to when the actual value indicates a high risk of developing sarcopenia, but the model predicts that the risk of developing sarcopenia is low. FP refers to that when the actual value indicates a low risk of developing sarcopenia, but the model predicts that the risk of developing sarcopenia is high. We use the above confusion matrix to calculate the model's accuracy, precision, specificity, and sensitivity using Eqs. (12) to (15).

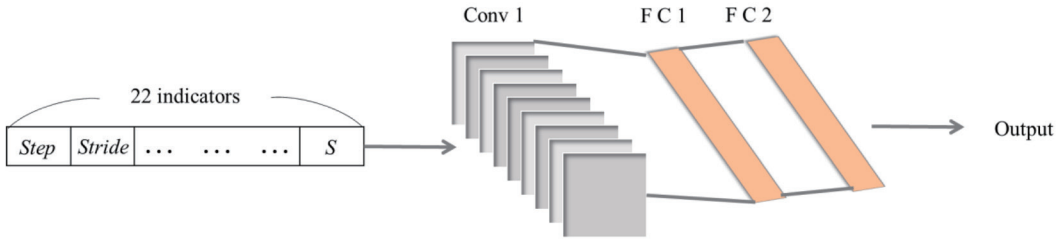

Fig. 7. (Color online) LCNet architecture.

$$Accuracy = \frac{TP + TN}{TP + TN + FP + FN} \tag{12}$$

$$Precision = \frac{TP}{TP + FP} \tag{13}$$

$$Specificity = \frac{TN}{TN + FP} \tag{14}$$

$$Sensitivity = \frac{TP}{TP + FN} \tag{15}$$

We use the DBA algorithm to augment the collected data to generalize the model's classification ability to various gaits during the model training. Table 2 shows the testing confusion matrix without and with data augmentation. The model's testing precision before data augmentation only reaches 82.61% in the classification of sarcopenia. In contrast, the model's testing precision after data augmentation is 91.58%, which means that the LCNet model has a strong generalization ability for different subjects. Additionally, it proves that data augmentation can greatly improve the model's classification ability. We use binary cross entropy as the loss function of LCNet, train with 30 batches, and finally, stop at 3500 epochs, and the accuracy of the model reaches 94.41%, which means that the LCNet model is effective in classifying the risk of developing sarcopenia. The specificity is 95.81%, indicating that the LCNet model is less likely to misjudge the subject as having a higher risk of sarcopenia. Finally, the sensitivity is 91.58%, which means that the LCNet model is less likely to miss patients with a high risk of developing sarcopenia. Figure 8 shows the indicators which were calculated from the confusion matrix without and with data augmentation. In the future, we hope to collect the data of the subjects during the Chair Stand Test, to increase the data that can be used to assess muscle strength in the training dataset, and to reduce the probability of misjudgment of sarcopenia patients. These results demonstrate that the data collected by the wearable device proposed in this study can be used to successfully classify the risk of developing sarcopenia by using the Bodi algorithm to calculate the indicators.

4.2 MSM evaluation design

In this section, we verify that the MSM proposed in this study can obtain more comprehensive performance for gait classification, so that its use can be extended to various other fields. To achieve this outcome, we input the gait parameter obtained by MSM into the model and compare it with the prediction results from the model whose only inputs are the data from the EAG. Table 3 shows the confusion matrix after only inputting the three-axis acceleration signals into the model and the confusion matrix after only inputting the EMG signals into the model. According to the confusion matrix shown in Tables 2 and 3, the results predicted by combining the three-axis acceleration and EMG signals can obtain better performance when classifying the

Table 2
Testing confusion matrix.

	Prediction			
	Without Data Augmentation		With Data Augmentation	
Actual	High risk of sarcopenia	Low risk of sarcopenia	High risk of sarcopenia	Low risk of sarcopenia
High risk of sarcopenia	19	3	87	8
Low risk of sarcopenia	4	40	8	183

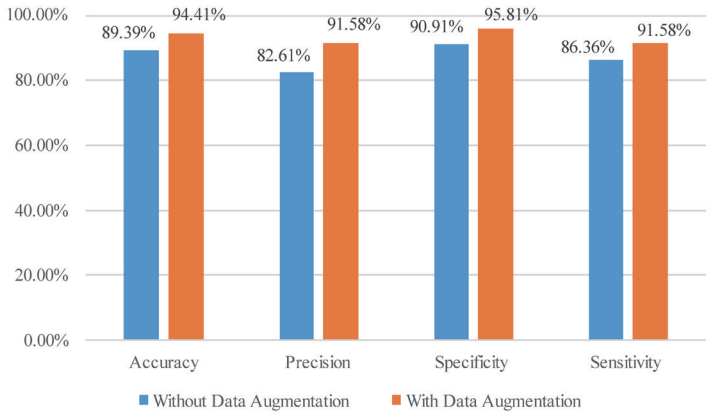

Fig. 8. (Color online) Indicators calculated from confusion matrix without and with data augmentation.

risk of sarcopenia. These results prove that the MSM proposed in this study can effectively obtain gait performance and the changes in muscle strength during human activity. Figure 9 shows the indicators which were calculated from the confusion matrix of the model that only uses three-axis acceleration signals and only uses EMG signals for training.

5. Discussion

In this study, we discuss the location and combination of sensors, data sampling rate, and statistical analysis.

5.1 Location and combination of sensors

During the test, the subject may be affected by the wearable device's large size, which may affect the way the subject walks or exercises, causing the data collected during the test to deviate from the patient's actual gait. The size of the MSM proposed in this study is approximately 7 × 5 × 2 cm^3, which is smaller than that of the wearable device proposed in related work,[31] and it can prevent the subject from changing the size of the device during the test. The subject will feel discomfort when wearing the device on the body or be inconvenienced when walking.

There is current literature indicating the use of a mobile phone to collect human gait data.[25] The mobile phone is convenient to wear, but it can only be worn on the left or right side of the

Table 3
Confusion matrix of the model.

	Prediction			
	Only Uses Three-Axis Acceleration Signals for Training		Only Uses EMG Signals for Training	
Actual	High risk of sarcopenia	Low risk of sarcopenia	High risk of sarcopenia	Low risk of sarcopenia
High risk of sarcopenia	77	18	80	15
Low risk of sarcopenia	16	175	14	177

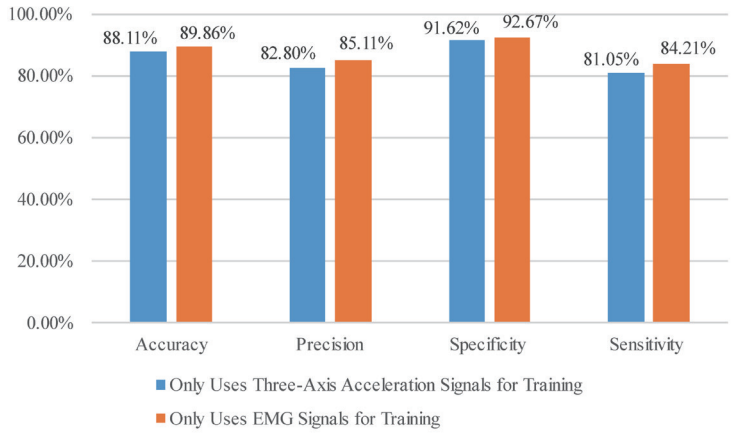

Fig. 9. (Color online) Indicators calculated from the confusion matrix of the model that only uses three-axis acceleration signals and only uses EMG signals for training.

human body; additionally, the wearing position is not uniform or fixed. This method may be affected by the subject's asymmetry while walking. In this study, according to human gait kinematics,[2] the proposed MSM is worn on the left and right erector spinae and at the back of the left and right calves in a symmetrical manner to obtain human gait cycle data, and information about the symmetry of the human body can therefore be effectively obtained.

In addition, to prove that both MSM and this device location can more accurately obtain the relevant gait parameter of the human body during walking and other activities, we use the step length obtained in this study to calculate additional indicators.[32] We adopt two evaluation indicators to compare, namely, MAPE and RMSE. The larger the value of MAPE, the closer the prediction is to reality; the larger the value of RMSE, the greater the error between the prediction and the reality. Table 4 shows the errors calculated for both step size and stride. The results demonstrate that the method proposed in this study performs better in terms of both MAPE and RMSE.

5.2 Data sampling rate

To obtain a higher accuracy, we test different sampling rates. We first test a sampling rate of 100 Hz and then decrease that value to 5 Hz. We can obtain 10 data points using a sampling rate of 100 Hz, and the number varies with different sampling rates. Figure 10 shows that when using a high sampling rate, it is easy to cause rapid battery power consumption and affect the overall

Table 4
Comparison of errors in step and stride.

	Step		Stride	
	MAPE (%)	RMSE (cm)	MAPE (%)	RMSE (cm)
Our proposed method	6.73	3.86	6.06	5.28
An *et al.*[32]	5.49	4.08	4.17	6.30

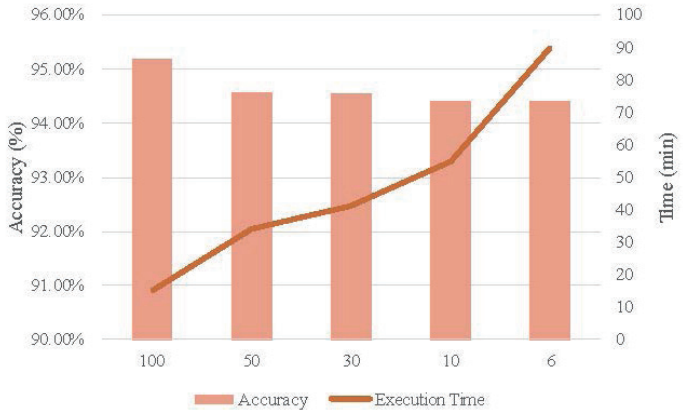

Fig. 10. (Color online) Relationship between sensor sampling rate and battery execution time.

performance of the hardware device. When the sampling rate is 6 Hz, the model's classification accuracy is not significantly reduced, and the working time of the 3.7 V lithium battery can be up to 1.5 h. Additionally, its stability is the best at a sampling rate of 6 Hz. Since it takes an hour to collect gait data, we adopt 6 Hz as the data sampling rate.

5.3 Statistical analyses

To understand the effects of different individuals on the asynchrony indicators, we adopt statistical analysis methods to explore the effects of gender, age, BMI, and the risk of sarcopenia.

5.3.1 Relationship between gender and other indicators

Men and women have different physiological structures. For example, there are usually differences in muscle strength between women and men. Therefore, we analyze the gait indicators from the Four-meter Usual Walking Speed Test and Time-up and Go Test for men and women, and the analysis results are shown in Table 5. We found that during the entire Four-meter Usual Walking Speed Test, which involves only standing or walking, men and women had significantly different waist force levels during walking. When compared with the Four-meter Usual Walking Speed Test, the Time-up and Go Test involves more movements, including standing, sitting, and turning back to walk. These movements require more muscle strength to support the body and maintain body balance. In Table 5, we can see that men and women have different degrees of waist exertion. The results also show that there are significant differences in

Table 5
(Color online) Independently sampled *T*-test applied to various indicators and gender in Four-meter Usual Walking Speed Test and Time-up and Go Test.

Result of Bodi algorithm	Four-meter Usual Walking Speed Test					Time-up and Go Test				
	Male (N=21)		Female (N=19)		p-value	Male (N=21)		Female (N=19)		p-value
	Mean	STD	Mean	STD		Mean	STD	Mean	STD	
Step	0.63	0.25	0.67	0.24	0.195	0.63	0.30	0.62	0.28	0.824
Stride	1.27	0.50	1.34	0.48	0.195	1.26	0.59	1.25	0.56	0.824
Num	7.89	3.11	7.40	2.77	0.150	8.48	3.86	8.41	3.62	0.876
Speed	52.34	11.87	47.66	37.01	0.172	20.95	31.16	10.34	104.88	0.209
TA_{Right_Leg}	1.09	0.11	1.12	0.14	0.078	1.10	0.10	1.10	0.12	0.622
TA_{Left_Leg}	1.10	0.11	1.11	0.13	0.311	1.11	0.13	1.09	0.12	0.174
TA_{Right_Waist}	1.02	0.27	1.02	0.27	0.838	1.02	0.02	1.02	0.02	0.316
TA_{Left_Waist}	1.02	0.27	1.01	0.26	0.125	1.01	0.02	1.01	0.02	0.793
$RMS_{ACC\_Right\_Waist}$	0.00	0.00	0.52	6.68	0.304	0.00	0.00	1.34	16.83	0.373
$RMS_{ACC\_Left\_Waist}$	0.00	0.00	0.47	6.05	0.380	0.00	0.00	1.40	17.57	0.374
$\overline{EMG}_{Right\_Leg}$	335.76	97.59	337.13	85.51	0.897	304.81	121.73	335.86	85.09	0.015
$\overline{EMG}_{Left\_Leg}$	303.40	9.30	300.60	21.61	0.128	302.92	12.19	303.43	17.20	0.776
$\overline{EMG}_{Right\_Waist}$	270.53	8.83	272.77	12.07	0.079	272.27	2.89	273.65	7.79	0.034
$\overline{EMG}_{Left\_Waist}$	267.75	80.51	206.80	122.05	<0.001	267.59	80.70	210.87	123.58	0.034
$RMS_{EMG\_Right\_Leg}$	341.04	103.15	343.66	93.37	0.819	310.87	124.92	341.92	1.39	0.019
$RMS_{EMG\_Left\_Leg}$	304.80	6.48	303.44	16.00	0.311	304.69	8.30	305.62	12.94	0.480
$RMS_{EMG\_Right\_Waist}$	268.57	80.49	211.93	121.71	<0.001	268.64	80.72	214.78	124.20	<0.001
$RMS_{EMG\_Left\_Waist}$	271.46	5.11	273.38	9.21	0.035	272.37	2.49	274.00	6.74	0.004
S_{ACC_Leg}	0.04	0.05	0.05	0.67	0.266	0.03	0.04	0.03	0.04	0.741
S_{ACC_Waist}	0.02	0.03	0.02	0.03	0.652	0.02	0.01	0.02	0.01	0.728
S_{EMG_Leg}	0.26	0.29	0.26	0.26	0.930	0.37	0.39	0.25	0.39	0.002
S_{EMG_Waist}	0.24	0.48	0.57	0.73	<0.001	0.23	0.48	0.56	0.48	<0.001

EMG indicators between the genders on the right side of the body, which means that men and women exhibit different degrees of deviation from their centers of weight during the test. Among them, women rely more on the muscle strength on the right side of the body to maintain balance than men do. This inference proves that men and women do have differences in muscle strength.

5.3.2 Relationship between age and other indicators

With increasing age, the skeletal muscle mass decreases each year. Starting from about 40 years of age, the skeletal muscle mass decreases by about 8% every ten years.[33] Therefore, we set the age of 40 as the demarcation point, and the analysis results are shown in Table 6. In the Four-meter Usual Walking Speed Test, the test distance is shorter, so it tests the subject's muscle power. However, young adults are stronger than elderly people, so in terms of walking speed and EMG-related indicators, age differences produce significant differences. In the Time-up and Go Test, the subjects must move from a sitting posture to a standing posture, which tests the subjects' physical balance and muscle endurance. However, elderly people have a poor physical balance due to muscle tissue degradation. Most elderly people reduce their walking speed to increase their walking stability. Therefore, there are significant differences in average acceleration, symmetry, and EMG-related indicators, indicating that the gait data from the elderly and young are significantly different.

5.3.3 Relationship between BMI and other indicators

Owing to the subjects' disparity in height and weight, we explore the effects of different BMIs on gait indicators. First, we use the BMI conversion equation to convert the heights and weights of the subjects into BMI, and we then divide them into three groups, namely, underweight, standard, and overweight. Then, we use one-way analysis of variance (ANOVA) to explore the relationship between BMI and gait. Table 7 show that during both the Four-meter

Table 6
(Color online) Independently sampled T-test applied to various indicators and age in Four-meter Usual Walking Speed Test and Time-up and Go Test.

Result of Bodi algorithm	Four-meter Usual Walking Speed Test					Time-up and Go Test				
	Older than 40 (N=18)		Younger than 40 (N=32)		p-value	Older than 40 (N=18)		Younger than 40 (N=32)		p-value
	Mean	STD	Mean	STD		Mean	STD	Mean	STD	
Step	0.65	0.25	0.66	0.24	0.851	0.66	0.31	0.61	0.27	0.126
Stride	1.30	0.51	1.31	0.48	0.851	1.32	0.61	1.21	0.55	0.126
Num	7.69	3.02	7.55	2.87	0.686	8.26	3.99	8.54	3.56	0.536
Speed	41.12	44.34	54.38	13.29	0.003	21.38	6.88	11.10	102.54	0.169
TA_{Right_Leg}	1.11	0.12	1.11	0.14	0.967	1.11	0.12	1.09	0.11	0.117
TA_{Left_Leg}	1.12	0.13	1.10	1.12	0.272	1.13	0.14	1.09	0.11	0.007
TA_{Right_Waist}	1.02	0.03	1.02	0.03	0.576	1.02	0.01	1.02	0.02	0.043
TA_{Left_Waist}	1.01	0.03	1.02	0.03	0.297	1.01	0.02	1.01	0.02	0.514
$RMS_{ACC\_Right\_Waist}$	0.00	0.01	0.43	5.76	0.443	0.07	0.68	1.18	16.02	0.476
$RMS_{ACC\_Left\_Waist}$	0.00	0.00	0.43	5.76	0.441	0.07	0.65	1.23	16.72	0.474
$\overline{EMG}_{Right\_Leg}$	371.02	62.24	317.16	98.16	<0.001	375.83	69.45	293.00	106.96	<0.001
$\overline{EMG}_{Left\_Leg}$	299.89	16.31	302.83	18.18	0.165	298.98	15.75	305.60	14.51	<0.001
$\overline{EMG}_{Right\_Waist}$	271.22	10.65	272.17	11.00	0.465	272.15	3.58	273.59	7.29	0.056
$\overline{EMG}_{Left\_Waist}$	246.72	101.94	224.34	114.68	0.082	246.00	101.66	228.33	115.86	0.187
$RMS_{EMG\_Right\_Leg}$	377.14	76.30	323.11	102.70	<0.001	382.78	81.93	298.56	108.71	<0.001
$RMS_{EMG\_Left\_Leg}$	301.91	10.52	305.19	13.92	0.034	301.67	10.06	307.23	11.36	<0.001
$RMS_{EMG\_Right\_Waist}$	247.91	102.03	228.86	113.67	0.138	247.26	101.64	231.86	116.07	0.233
$RMS_{EMG\_Left\_Waist}$	272.30	7.16	272.73	8.16	0.646	272.27	3.23	273.90	6.28	0.012
S_{ACC_Leg}	0.04	0.05	0.04	0.06	0.802	0.04	0.05	0.03	0.04	0.001
S_{ACC_Waist}	0.02	0.02	0.02	0.03	0.999	0.02	0.02	0.02	0.02	0.144
S_{EMG_Leg}	0.24	0.14	0.27	0.32	0.174	0.25	0.17	0.33	0.37	0.008
S_{EMG_Waist}	0.36	0.61	0.48	0.67	0.109	0.35	0.61	0.47	0.68	0.121

Table 7
(Color online) One-way ANOVA applied to various indicators and BMI in Four-meter Usual Walking Speed Test and Time-up and Go Test.

Result of Bodi algorithm	Four-meter Usual Walking Speed Test								Time-up and Go Test							
	Overweight (O) (N=16)		Standard (S) (N=28)		Underweight (U) (N=6)		p-value	significant	Overweight (O) (N=16)		Standard (S) (N=28)		Underweight (U) (N=6)		p-value	significant
	Mean	STD	Mean	STD	Mean	STD			Mean	STD	Mean	STD	Mean	STD		
Step	0.64	0.25	0.66	0.25	0.66	0.20	0.703		0.63	0.29	0.63	0.29	0.62	0.27	0.973	
Stride	1.28	0.50	1.33	0.50	1.32	0.40	0.703		1.26	0.57	1.26	0.59	1.23	0.54	0.973	
Num	7.91	3.09	7.52	2.89	7.19	2.56	0.392		8.36	3.64	8.49	3.83	8.36	3.48	0.956	
Speed	41.30	48.10	54.16	11.99	50.66	8.00	0.002	S > O	10.89	76.88	21.14	51.88	4.38	1699.03	0.206	
TA_{Right_Leg}	1.11	0.14	1.12	0.13	1.09	0.11	0.432		1.08	0.09	1.11	0.12	1.10	0.12	0.193	
TA_{Left_Leg}	1.10	0.11	1.12	0.13	1.08	0.08	0.204		1.09	0.11	1.11	0.13	1.08	0.10	0.235	
TA_{Right_Waist}	1.02	0.03	1.02	0.03	1.03	0.23	0.524		1.02	0.02	1.02	0.02	1.02	0.03	0.429	
TA_{Left_Waist}	1.01	0.03	1.02	0.03	1.02	0.03	0.733		1.00	0.02	1.01	0.02	1.02	0.03	0.027	U > S > O
$RMS_{ACC\_Right\_Waist}$	0.02	0.18	0.53	6.80	0.00	0.00	0.686		0.08	0.72	1.34	17.13	0.00	0.00	0.692	
$RMS_{ACC\_Left\_Waist}$	0.02	0.18	0.48	6.16	0.00	0.00	0.687		0.08	0.69	1.40	17.88	0.00	0.00	0.690	
$\overline{EMG}_{Right\_Leg}$	344.57	80.44	326.79	102.85	360.75	29.85	0.071		332.22	100.49	309.10	11.66	361.77	33.37	0.011	U > S
$\overline{EMG}_{Left\_Leg}$	301.34	16.64	301.29	17.54	305.18	20.03	0.464		302.97	11.77	302.14	16.75	308.94	15.45	0.051	
$\overline{EMG}_{Right\_Waist}$	270.21	10.42	272.55	6.34	272.79	22.63	0.207		272.08	3.42	272.78	6.85	277.06	7.63	<0.001	U > S > O
$\overline{EMG}_{Left\_Waist}$	241.29	107.08	238.78	105.17	178.94	131.47	0.008	O > S > U	241.03	109.74	242.31	105.08	182.21	129.90	0.010	S > O > U
$RMS_{EMG\_Right\_Leg}$	351.29	90.34	333.60	109.41	361.12	29.88	0.174		339.22	110.09	315.69	114.69	362.86	32.50	0.030	U > O > S
$RMS_{EMG\_Left\_Leg}$	303.08	12.89	303.83	11.94	307.36	16.51	0.227		304.60	8.17	304.47	12.17	310.48	12.49	0.011	U > O > S
$RMS_{EMG\_Right\_Waist}$	242.38	107.02	242.30	105.03	187.25	128.81	0.018	O > S > U	242.46	109.46	244.68	105.39	189.94	131.97	0.023	S > O > U
$RMS_{EMG\_Left\_Waist}$	271.48	6.36	272.91	4.61	273.95	17.41	0.189		272.23	2.91	273.11	5.69	277.13	7.53	<0.001	U > S > O
S_{ACC_Leg}	0.04	0.06	0.05	0.06	0.05	0.07	0.463		0.03	0.03	0.04	0.05	0.02	0.04	0.172	
S_{ACC_Waist}	0.02	0.03	0.02	0.02	0.01	0.01	0.075		0.02	0.02	0.02	0.01	0.01	0.02	0.402	
S_{EMG_Leg}	0.23	0.19	0.29	0.33	0.20	0.09	0.047	S > O	0.27	0.24	0.34	0.37	0.19	0.08	0.011	S > O > U
S_{EMG_Waist}	0.40	0.63	0.39	0.62	0.76	0.77	0.007	U > S > O	0.40	0.65	0.38	0.62	0.72	0.79	0.016	U > O > S

Usual Walking Speed Test and Time-up and Go Test, the gait indicators collected from different body parts are significantly related to BMI; however, there is no regularity. Finally, there is no significant difference between BMI and gait indicators.

5.3.4 Relationship between risk of developing sarcopenia and other indicators

When a human is walking or standing, the waist muscles must be used for support, and it requires additional leg strength to get up. However, people at a higher risk of sarcopenia have a lower muscle mass than those at a lower risk. Therefore, we explore the relationship between the risk of developing sarcopenia and other indicators, and the results are shown in Table 8. Since

Table 8
(Color online) Independently sampled T-test applied to various indicators and the risk of sarcopenia in Four-meter Usual Walking Speed Test and Time-up and Go Test.

Result of Bodi algorithm	Four-meter Usual Walking Speed Test					Time-up and Go Test				
	High risk (N=16)		Low risk (N=36)		p-value	High risk (N=16)		Low risk (N=36)		p-value
	Mean	STD	Mean	STD		Mean	STD	Mean	STD	
Step	0.67	0.25	0.65	0.24	0.458	0.63	0.29	0.63	0.29	0.975
Stride	1.34	0.49	1.30	0.48	0.458	1.26	0.57	1.25	0.58	0.975
Num	7.46	2.94	7.67	2.91	0.556	8.40	3.72	8.46	3.73	0.896
Speed	44.04	47.84	52.26	13.00	0.101	12.90	103.81	15.69	70.47	0.784
TA_{Right_Leg}	1.12	0.13	1.11	0.13	0.448	1.11	0.13	1.09	0.11	0.233
TA_{Left_Leg}	1.13	0.14	1.10	0.11	0.093	1.11	0.14	1.10	0.12	0.280
TA_{Right_Waist}	1.02	0.03	1.02	0.03	0.152	1.02	0.02	1.02	0.02	0.844
TA_{Left_Waist}	1.02	0.03	1.02	0.03	0.251	1.01	0.02	1.01	0.02	0.093
$RMS_{ACC\_Right\_Waist}$	0.01	0.08	0.44	6.17	0.495	0.12	0.79	1.09	15.54	0.541
$RMS_{ACC\_Left\_Waist}$	0.11	0.09	0.40	5.59	0.496	0.11	0.77	1.14	16.22	0.538
$\overline{EMG}_{Right\_Leg}$	340.52	89.40	334.68	91.35	0.603	341.51	80.49	314.03	111.21	0.016
$\overline{EMG}_{Left\_Leg}$	300.62	22.44	302.32	14.75	0.500	304.96	17.89	302.40	13.85	0.177
$\overline{EMG}_{Right\_Waist}$	273.14	9.02	271.21	11.60	0.151	272.93	8.66	273.14	4.73	0.823
$\overline{EMG}_{Left\_Waist}$	194.63	126.63	250.18	97.60	<0.001	195.85	125.22	252.97	98.97	<0.001
$RMS_{EMG\_Right\_Leg}$	345.43	96.45	341.21	98.11	0.727	344.81	86.47	321.38	115.75	0.052
$RMS_{EMG\_Left\_Leg}$	303.93	16.50	304.05	10.80	0.946	306.99	14.11	304.40	9.49	0.062
$RMS_{EMG\_Right\_Waist}$	200.75	126.27	252.17	97.24	0.001	202.39	126.86	254.35	98.83	<0.001
$RMS_{EMG\_Left\_Waist}$	273.77	6.86	272.02	8.16	0.054	273.42	7.02	273.26	4.52	0.839
S_{ACC_Leg}	0.04	0.06	0.04	0.06	0.999	0.04	0.05	0.03	0.03	0.114
S_{ACC_Waist}	0.02	0.02	0.02	0.03	0.219	0.01	0.01	0.02	0.02	0.343
S_{EMG_Leg}	0.28	0.29	0.25	0.27	0.479	0.24	0.20	0.33	0.35	0.005
S_{EMG_Waist}	0.64	0.75	0.34	0.58	<0.001	0.63	0.76	0.33	0.58	0.001

the Time-up and Go test requires that the subject moves from a sitting posture to a standing posture, the waist EMG-related indicators in this test are significantly different from those in the Four-meter Walking test. There are also significant differences in the EMG-related indicators from the legs.

From the above statistical analysis, we observe that the differences in gender, age, and the risk of developing sarcopenia are related to significant differences in EMG in gait indicators. In other words, the EMG signals will be different for men and women, the elderly and young adults, and those at high and low risks of developing sarcopenia. In addition, we can see that there is a significant difference between age and acceleration. Therefore, the gait indicators that we use can effectively classify the risk of developing sarcopenia, and the training dataset includes information about the above factors, which can improve the model's generalization ability.

6. Conclusion

Wearable sensors are often used to obtain gait information during human activities. However, most of the measurements are performed using a single inertial sensor. Such a sensor may not notice changes in muscle strength, which are closely related to many diseases. Therefore, we propose a wearable hardware device that combines an inertial sensor with a biomedical signal sensor, which can be used to obtain gait information and the change in muscle strength during human activities. Next, we calculate important gait parameters using the Bodi algorithm and then input those parameters into the LCNet model to classify the risk of sarcopenia. In the future, we hope to obtain more gait information and apply our proposed MSM to different medical fields such as scoliosis, Parkinson's disease, and multiple sclerosis.

References

1 S. Díaz, J. B. Stephenson, and M. A. Labrador: Appl. Sci. **10** (2020) 234. https://doi.org/10.3390/app10010234
2 W. Tao, T. Liu, R. Zheng, and H. Feng: Sensors **12** (2012) 2255. https://doi.org/10.3390/s120202255
3 A. S. Alharthi, S. U. Yunas, and K. B. Ozanyan: IEEE Sens. J. **19** (2019) 9575. https://ieeexplore.ieee.org/document/8762100
4 Y. Zhang, W. Yan, Y. Yao, J. B. Ahmed, Y. Tan, and D. Gu: IEEE Trans. Neural Syst. Rehabilit. Eng. **28** (2020) 591. https://ieeexplore.ieee.org/abstract/document/8970522
5 A. A. Ibrahim, A. Küderle, H. Gaßner, J. Klucken, B. M. Eskofier, and F. Kluge: J. NeuroEng. Rehabilit. **17** (2020) 165. https://doi.org/10.1186/s12984-020-00798-9
6 A. J. Cruz-Jentoft, G. Bahat, J. Bauer, Y. Boirie, O. Bruyère, T. Cederholm, C. Cooper, F. Landi, Y. Rolland, A. A. Sayer, S. M. Schneider, C. C. Sieber, E. Topinkova, M. Vandewoude, M. Visser, and M. Zamboni: Age and ageing, **48** (2019) 16. https://www.ncbi.nlm.nih.gov/pmc/articles/PMC6322506/
7 L. Chen, J. Woo, P. Assantachai, T. Auyeung, M. Chou, K. Iijima, H. C. Jang, L. Kang, M. Kim, and S. Kim: JAMDA **21** (2020) 300. https://doi.org/10.1016/j.jamda.2019.12.012
8 J. Joshua, C. Qian, P. Valentin, J. A. Krishnan, and S. Bruce: Telemed. J. E. Health, **20** (2014) 1035. https://pubmed.ncbi.nlm.nih.gov/24694291/
9 X. Liu, C. Zhao, B. Zheng, Q. Guo, X. Duan, A. Wulamu, and D. Zhang: Front. Comput. Sci. **3** (2021) 42. https://www.frontiersin.org/articles/10.3389/fcomp.2021.661676/full
10 A. Muro-de-la-Herran, B. Garcia-Zapirain, and A. Mendez-Zorrilla, Sensors **14** (2014) 3362. https://doi.org/10.3390/s140203362
11 T. Gujarathi and K. Bhole: Communication and Networking Technologies (ICCCNT) (2019) 1–5. https://ieeexplore.ieee.org/document/8944545
12 S. Tian, Y. Liu, L. Li, W. Fu, and C. Peng: J. Biomech. **43** (2010) 551. https://doi.org/10.1016/j.jbiomech.2009.09.034
13 K. Kashiwagi, T. Nakakuki, and C. Ishii: 2011 50th IEEE Conf. Decision and Control and European Control Conference, (2011) 3204–3209. https://ieeexplore.ieee.org/document/6160838
14 A. Bonetto and L. F. Bonewald: Basic and Appl. Bone Biol. (2019) 317. https://doi.org/10.1016/B978-0-12-813259-3.00016-6
15 D. Alvarez, R. C. Gonzalez, A. Lopez, and J. C. Alvarez: 2006 Int. Conf. IEEE Engineering in Medicine and Biology Society, (2006) 5964–5967. https://ieeexplore.ieee.org/document/4463166
16 Y. Jin, H. Toh, W. Soh, and W. Wong: 2011 IEEE Int. Conf. Pervasive Computing and Communications (PerCom), (2011) 222–230. https://ieeexplore.ieee.org/document/5767590
17 H. Lan, C. Yu, and N. El-Sheimy: China Satellite Navigation Conf. (CSNC) **342** (2015) 677. https://link.springer.com/chapter/10.1007%2F978-3-662-46632-2_59
18 H. U. Kuriki, F. M. D. Azevedo, L. S. O. Takahashi, E. M. Mello, R. D. F. N. Filho, and N. Alves: EMG Methods for Evaluating Muscle and Nerve Function (2012) pp. 31–54. https://scholar.google.com.tw/scholar?q=The+Relationship+Between+Electromyography+and+Muscle+Force&hl=zh-TW&as_sdt=0&as_vis=1&oi=scholart
19 T. Zebin, M. Sperrin, N. Peek, and A. J. Casson: 2018 40th Annu. Int. Conf. IEEE Engineering in Medicine and Biology Society (EMBC) (2018) 1–4. https://ieeexplore.ieee.org/document/8513115
20 U. Côté-Allard, C. K. Fall, A. Drouin, A. Campeau-Lecours, C. Gosselin, K. Glette, F. Laviolette, and B. Gosselin: IEEE Trans. Neural Syst. Rehabil. Eng. **27** (2019) 760. https://ieeexplore.ieee.org/document/8630679/authors
21 H. I. Fawaz, G. Forestier, L. Idoumghar, and P. Muller: ArXiv 2018. https://arxiv.org/abs/1808.02455
22 G. Forestier, F. Petitjean, H. A. Dau, G. I. Webb, and E. Keogh: 2017 IEEE Int. Conf. Data Mining (ICDM) (2017) 865–870. https://ieeexplore.ieee.org/document/8215569
23 B. K. Iwana and S. Uchida: ArXiv **16** (2020) 1–32. https://doi.org/10.1371/journal.pone.0254841
24 K. Benio, M. Toshio, and K. Motoki: Gait & Posture **94** (2021) 230. https://doi.org/10.1016/j.gaitpost.2021.04.006
25 Q. Zou, Y. Wang, Z. Yi, W. Qian, and S. Chao: IEEE Trans. Information Forensics and Security **15** (2020) 3197. https://doi.org/10.1109/TIFS.2020.2985628
26 K. Suzuki, M. Niitsu, T. Kamo, S. Otake, and Y. Nishida: Open Journal of Therapy and Rehabilitation, **7** (2019) 79. https://doi.org/10.4236/ojtr.2019.73005
27 M. M. Erdem, G. Koc, K. Kismet, C. Yasti, and S. Topuz: Burns **46** (2020) 897. https://doi.org/10.1016/j.burns.2019.10.022
28 R. Singh, K. Iqbal, G. White, and J. Holtz: Machine Learning in Medicine and Biology (2019) 1–22. https://www.intechopen.com/chapters/65853

29 L. Xu, X. Chen, S. Cao, X. Zhang, and X. Chen: Sensors **18** (2018) 3226. http://dx.doi.org/10.3390/s18103226
30 P. Sarkar and A. Etemad: IEEE Trans. Affective Computing (accessed August 2020). https://arxiv.org/abs/2002.03898v2
31 Q. Zou, Y. Wang, Q. Wang, Y. Zhao, and Q. Li: IEEE Trans. Inf. Forensics and Security **15** (2020) 3197. https://doi.org/10.1109/TIFS.2020.2985628
32 S. An, Y. Tuncel, G. K. Krishnakumar, G. Bhat, and U. Ogres: Signal Processing (accessed September 2021). https://arxiv.org/abs/2102.11895
33 R. R. Kalyani, M. Corriere, and L. Ferrucci: Lancet Diabetes Endocrinol. **2** (2014) 819. https://doi.org/10.1016/s2213-8587(14)70034-8

About the Authors

I-Miao Chen graduated from the Department of Medical Informatics of Chung Shan Medical University. She specializes in medical image processing, medical health care, and signal processing through artificial intelligence or deep learning and has several publications in high-impact journals.

Pin-Yu Yeh graduated from the Department of Medical Informatics of Chung Shan Medical University. Most of her research is related to medical imaging, deep learning, and health care.

Ting-Chi Chang graduated from the Department of Medical Informatics of Chung Shan Medical University. She is interested in the research direction of deep learning, image processing, and signal processing. She specializes in medical or health care research combined with deep learning and has several publications in high-impact journals.

Ya-Chu Hsieh graduated from the Department of Medical Informatics of Chung Shan Medical University. Among her research interests are signal processing, image processing, deep learning, and artificial intelligence. She specializes in medical research combined with deep learning and has several publications in high-impact journals.

Chiun-Li Chin is an associate professor at the Department of Medical Informatics of Chung Shan Medical University. His research focuses on signal processing, image processing, deep learning, and artificial intelligence. He has many innovative ideas and puts them into practice in competitions or published papers. He has won the National Innovation Award given by Research Center for Biotechnology and Medicine Policy (RBMP).